https://doi.org/10.46813/2024-154-020

DIFFERENT APPROACHES FOR DESCRIPTION OF NEGATIVE ION FORMATION IN AN ARGON/ACETYLENE PLASMA AFTERGLOW

I.B. Denysenko[1], N.A. Azarenkov[1,2], V. Vinnichenko[1], G. Burmaka[1]

[1]V.N. Karazin Kharkiv National University, Kharkiv, Ukraine;
[2]National Science Center "Kharkiv Institute of Physics and Technology", Kharkiv, Ukraine

E-mail: idenysenko@yahoo.com

Properties of an Ar/C_2H_2 plasma afterglow with dust particles are investigated at different assumptions concerning negative ion formation. First, numerical calculations are carried out assuming that $C_{2n}H_2^-$ negative ions, where *n* is a natural number, are the dominant anions in the plasma afterglow (the case (i)). Second, the studies are conducted assuming that $C_{2n}H^-$ anions are only the negative ions, which are present in the afterglow plasma (the case (ii)). It is shown that the total density of negative ions n_- in the case (ii) is smaller than n_- in the case (i). Due to smaller n_-, the positive ion densities are smaller and the absolute values of the mean dust charge and its variances are larger in the case (ii) than the corresponding values calculated using the approach (i). We also calculated the dust charge distribution functions (DCDFs) for late afterglow times. It is found that the DCDFs obtained in the case (ii) are shifted to the region of larger negative charges comparing with the dust charge distributions obtained in the case (i). The differences are mainly due to the loss of $C_{2n}H^-$ anions in collisions with H atoms in the case (ii). In the case when the loss of negative ions in collisions with H atoms is not taken into account in the models, the both approaches give nearly the same time dependences for positive and negative ion densities, electron density, mean dust charge and its variance.

PACS: 52.27.Lw, 52.25.Vy, 52.65.-y, 52.50.Dg

INTRODUCTION

Hydrocarbon plasmas have been widely attracted attention of researchers because these plasmas are used for formation of carbon and hydrocarbon nanostructures [1-3]. Negative ion reactions are usually not incorporated in the modelling of hydrocarbon discharges used for formation of carbon nanotubes and other vertically aligned carbon nanostructures [1, 2]. While analysing the carbonaceous dust generation in plasma, many authors have focused their attention on negative ions because reactions of anions with neutral molecules can lead to the generation of the dust particles [4]. In models of many authors, it was assumed that the primary C_2H^- anions, formed through the electron impact dissociative attachment on C_2H_2, can trigger a consecutive chain of polymerization reactions that generally evolves as follows: $C_2H^- + C_2H_2 \rightarrow C_4H^- + H_2$, $C_4H^- + C_2H_2 \rightarrow C_6H^- + H_2$,…, $C_{2n}H^- + C_2H_2 \rightarrow C_{2n+2}H^- + H_2$, where *n* is a natural number, and it is commonly referred to as the Winchester mechanism [4]. In [5], some new mechanisms for anion formation were proposed: the generation of branched (and probably vibrationally excited) molecules $C_{2n}H_2^*$ and subsequent enhanced dissociative electron attachment to form $C_{2n}H^-$ anions; the formation of the vinylidene anion (H_2CC^-) and the consecutive chain of polymerization reactions to form $C_{2n}H_2^-$ and $C_{2n}H_4^-$. In [5], anions with different number of hydrogen atoms (k_H =1, 2. and 4) were considered. In [6], it was assumed that only negative ions with k_H = 2 can be generated in Ar/C_2H_2 plasma, while in [7], it was suggested that the growth of anion clusters takes place in the reactions: $e + C_2H_2 \rightarrow C_2H^- + H$, $C_2H^- + C_2H_2 \rightarrow C_2H_2^- + C_2H$,…, $C_{2n}H_2^- + C_2H_2 \rightarrow C_{2n+2}H_2^- + H_2$. The same mechanism of formation of large anions was assumed in our previous work [8]. In [7], positive and negative ion distributions were measured in the steady state of an Ar/C_2H_2 discharge, and a volume averaged kinetic model for this plasma was developed which was able to satisfactory reproduce the experimental results. However, in [9], it was noted that signals attributed previously to $C_{2n}H_2^-$ anions [7] should be mostly assigned to the contribution of $C_{2n-1}N^-$ anions. This is because the bottle of C_2H_2 contained an unexpected 6.3% of N_2 as impurity in the experiment, much more than the commercially specified limit (N_2 < 0.4%). The results presented in [9] again raised the question of whether vinylidene anion (H_2CC-) plays a key role in the initiation of the polymerization chain.

In this paper, we check how properties of an Ar/C_2H_2 plasma afterglow depend on the pathway of formation of hydrocarbon anions. The case when the afterglow plasma contains dust particles (with the dust charge density smaller when the densities of main ions) is considered. The time dependences for the electron and ion densities, dust charge and its variance and the dust charge distribution function (DCDF), which are calculated using the reactions described in [8] (in [8], $C_{2n}H_2^-$ anions are assumed to be the dominant negative ions), are compared with those calculated assuming that there is formation of only $C_{2n}H^-$ anions in the Ar/C_2H_2 plasma afterglow. It is also analyzed how interaction of anions with hydrogen atoms affects the densities of negative ions and other plasma species.

1. MODEL

We consider a gas-discharge plasma of radius R = 15 cm and height L = 7 cm sustained in a mixture of argon and acetylene. As in the case considered in [8], it is assumed that the discharge consists of electrons with density n_e and temperature T_e, eleven positive ions (Ar^+, ArH^+, C_2H^+, $C_2H_2^+$, $C_4H_2^+$, $C_6H_4^+$, $C_8H_6^+$, $C_{10}H_6^+$, $C_{12}H_6^+$, $C_{14}H_8^+$, $C_{16}H_8^+$), four nonradical neutrals (Ar, C_2H_2, H_2, C_4H_2) and two radicals (C_2H and H), argon atoms in the ground state (Ar_0) with density n_{Ar}, metastable argon atoms (Ar_m) with density n_m, argon atoms in the resonance 4s states ($^3P_1$ and $^1P_1$) (Ar_r) with density n_r as well as argon atoms in 4p states (Ar(4p)) with density n_{4p}. We also assume that the plasma contains negative ions and consider two possible compositions of negative ions. In *the case (i)*, it is assumed that there are the following negative ions: C_2H^-, H_2CC^-, $C_4H_2^-$, $C_6H_2^-$, $C_8H_2^-$, $C_{10}H_2^-$ and $C_{12}H_2^-$ [7]. The reactions with participation of negative ions taken into account in the model in the case (i) are the same as in our previous paper [8] and are shown in Table 1.

Table 1

Collisional processes for the production and loss of negative ions taken into account in this model in the case (i)

	Reaction, rate constant (cm^3/s)	Ref.
(R1)	$e + C_2H_2 \rightarrow C_2H^- + H$ $9.27\cdot10^{-12}T_e^{-0.84}\exp(-2.51/T_e)$	[7]
(R2)	$C_mH_n^- + Ar^+ \rightarrow C_mH_n + Ar$, $1.01\cdot10^{-7}$	[10]
(R3)	$C_mH_n^- + C_lH_k^+ \rightarrow C_mH_n + C_lH_k$, $5.0\cdot10^{-8}$	[5]
(R4)	$C_mH_n^- + ArH^+ \rightarrow C_mH_n + H + Ar$, $3.0\cdot10^{-8}$	[4,10]
(R5)	$C_2H^- + C_2H_2 \rightarrow C_2H_2^- + C_2H$, $3.5\cdot10^{-11}$	[7]
(R6)	$C_{2n}H_2^- + C_2H_2 \rightarrow C_{2n+2}H_2^- + H_2$, $1.0\cdot10^{-12}$	[4]
(R7)	$C_2H^- + H \rightarrow C_2H_2 + e$, $1.6\cdot10^{-9}$	[11]

Table 2

Collisional processes associated with negative ions and taken into account in this model in the case (ii)

	Reaction, rate constant (cm^3/s)	Ref.
(R8)	$e + C_2H_2 \rightarrow C_2H^- + H$ $9.27\cdot10^{-12}T_e^{-0.84}\exp(-2.51/T_e)$	[7]
(R9)	$C_{2n}H^- + C_2H_2 \rightarrow C_{2n+2}H^- + H_2$, $1.0\cdot10^{-12}$, n =1- 5	[4]
(R10)	$C_mH_n^- + Ar^+ \rightarrow C_mH_n + Ar$, $1.01\cdot10^{-7}$	[10]
(R11)	$C_mH_n^- + C_lH_k^+ \rightarrow C_mH_n + C_lH_k$, $5.0\cdot10^{-8}$	[5]
(R12)	$C_mH_n^- + ArH^+ \rightarrow C_mH_n + H + Ar$, $3.0\cdot10^{-8}$	[10]
(R13)	$C_2H^- + H \rightarrow C_2H_2 + e$, $1.6\cdot10^{-9}$	[11]
(R14)	$C_4H^- + H \rightarrow C_4H_2 + e$, $8.3\cdot10^{-10}$	[11]
(R15)	$C_{2n}H^- + H \rightarrow C_{2n}H_2 + e$, $5.0\cdot10^{-10}$, n =3, 4, 5, 6	[11]

Since the presence of negative ions with two hydrogen atoms in a large amount in Ar/C_2H_2 plasma is questionable [9], the calculations were also carried out assuming that the plasma contains only negative ions with a single atom of hydrogen [4]: C_2H^-, C_4H^-, C_6H^-, C_8H^-, $C_{10}H^-$, and $C_{12}H^-$ [*the case (ii)*]. The collisional reactions connected with the production and loss of negative ions in the case (ii) are presented in Table 2.

The reaction rates for the interaction of C_2H^-, C_4H^- and C_6H^- with H atoms are taken from [11]. The rates for interaction of C_8H^-, $C_{10}H^-$, and $C_{12}H^-$ with hydrogen atoms are assumed to be the same as for the interaction of C_6H^- with H [11].

We also assume that the gas discharge plasma contains dust particles with radius a_d. However, it is assumed that the dust density is small, and the dust particles do not affect much on plasma characteristics. We also assume that the energy distributions for ions and electrons are Maxwellian, and that the positive ions and dust particles are at gas temperature T_g. The electron temperature T_e as a function of the afterglow time t for the initial stage of the afterglow is found from the power balance equation (Eq. (6) in [8]). In the plasma afterglow, it is additionally assumed that T_e cannot be smaller than an afterglow temperature T_{aft} assumed to be 0.3 eV, i.e. after its decay to reach T_{aft}, T_e becomes time-independent [8]. The gas temperature is assumed to be 0.0345 eV (400 K), as in [6, 7], while the temperature of negative ions T_- is assumed to be $3T_g$ [8]. Here, we present the results of our calculations for the conditions typical for the afterglow plasma experiments [8, 12]. In the case considered here, the dominant neutral species are argon atoms in the ground state and their density $n_{Ar} \approx P/(k_BT_g)$, where P = 10 Pa is the total gas pressure and k_B is the Boltzmann constant. In our model, the densities of acetylene molecules and electrons at t = 0 are input parameters. Here, we present the results for the case $n_{C2H2} = 5\cdot10^{13}$ cm^{-3} and $n_e(0) = 10^9$ cm^{-3} (the so-called case of large acetylene density and small n_e in [8]).

The density of a species X (electrons, H_2, C_4H_2, C_2H, H, argon atoms in excited states, as well as negative and positive ions, excepting of $C_{16}H_8^+$) is found from the balance equation

$$\partial n^{(X)}/\partial t = \sum_i R_{G,i}^{(X)} - \sum_i R_{L,i}^{(X)}, \qquad (1)$$

where $R^{(X)}_{G,i}$ and $R^{(X)}_{L,i}$ are, respectively, the rates for reactions describing generation and loss processes of the species X. The density of $C_{16}H_8^+$ ions is calculated from the quasineutrality condition

$$\sum_\alpha n_\alpha^+ = n_e + \sum_\alpha n_\alpha^-, \qquad (2)$$

where n_α^+ and n_α^- are, respectively, the densities of αth positive and negative ions.

Various processes for the loss and generation of the discharge species, including the collisional processes in the bulk plasma and the processes on plasma walls, are considered in this study. The processes and their rate coefficients are described in detail in our previous paper [8].

The mean dust charge Z_d as a function of time was found from the following expression

$$\frac{\partial Z_d}{\partial t} = \nu_{id} - \nu_{-d} - \nu_{ed}, \qquad (3)$$

where ν_{id}, ν_{-d}, and ν_{ed} are the mean frequencies with which a particle with charge Z_d collects positive ions, negative ions and electrons, respectively.

For $Z_d < 0$, $\nu_{ed} = a_d^2 n_e \sqrt{\frac{8\pi e T_e}{m_e}} \exp\left(\frac{\varphi_s}{T_e}\right)$,

$$\nu_{id} = a_d^2 \sum_j n_j^+ \sqrt{\frac{8\pi e T_+}{m_{j+}}} (1 - \xi\tau + H_z \xi^2 \tau^2 \lambda_s n_g \sigma_{ig}),$$

$$\nu_{-d} = a_d^2 \sum_j n_j^- \sqrt{\frac{8\pi e T_-}{m_{j-}}} \exp\left(\frac{\varphi_s}{T_-}\right),$$

where $\xi = \varphi_s/T_e$, $\tau = T_e / T_+$, $\varphi_s = eZ_d/a_d$, $\sigma_{ig} \approx 1/(n_g \lambda_{iav})$ is the average cross-section for ion–neutral collisions, e is the elementary charge, λ_{iav} is the average ion mean-free path and n_g ($\approx n_{Ar}$) is the total density of neutral species. Here, H_z is a coefficient which is a function of the ratio $|eZ_d/(\lambda_s T_+)|$ [12] and λ_s is the screening length, which is of the same order as the Debye length [13]. T_+ is the positive ion temperature. m_e, m_{j+} and m_{j-} are the masses of electrons, jth positive ions and jth negative ions, respectively.

For $Z_d > 0$, $\nu_{ed} = a_d^2 n_e \sqrt{8\pi e T_e/m_e}(1 + \varphi_s/T_e)$,

$\nu_{id} = a_d^2 \sum_j n_j^+ \sqrt{8\pi e T_+/m_{j+}} \exp(-\varphi_s/T_+)$ and

$\nu_{-d} = a_d^2 \sum_j n_j^- \sqrt{8\pi e T_-/m_{j-}} (1 + \varphi_s/T_-)$.

The charge distribution of dust particles can be well described by the Gaussian distribution [8, 14]:

$$F_{Gk} = \frac{1}{(2\pi\sigma_Z^2)^{\frac{1}{2}}} \exp\left[-\frac{(-Z_d^k + Z_d)^2}{2\sigma_Z^2}\right], \quad (4)$$

where Z_d is described by equation (3), $Z^k_d = ke$ and k is an integer. The variance σ^2_z as a function of time can be obtained from the following equation [8, 14]:

$$\frac{\partial \sigma_Z^2}{\partial t} \approx -\alpha_1' \sigma_Z^2 + \alpha_2, \quad (5)$$

where $\alpha'_1 = 2(\nu'_{ed} + \nu'_{-d} - \nu'_{id})$ with primes indicating derivatives with respect to Z_d, $\alpha_2 = \nu_{id} + \nu_{-d} + \nu_{ed}$.

The dust charge distribution function F_k can be also described by the following master equation [15]:

$$\frac{d}{dt} F_k = (\nu_{ed}^{k+1} + \nu_{-d}^{k+1}) F_{k+1} - (\nu_{ed}^k + \nu_{-d}^k + \nu_{id}^k) F_k + \nu_{id}^{k-1} F_{k-1}, \quad (6)$$

where ν^k_{ed}, ν^k_{id} and ν^k_{-d} are the frequencies with which a particle with charge Z^k_d collects electrons, positive ions and negative ions, respectively. The expressions for ν^k_{id}, ν^k_{-d} and ν^k_{ed} are coinciding with the corresponding expressions for ν_{id}, ν_{-d} and ν_{ed} if one replaces in these expressions Z_d by Z^k_d [8]. The DCDF has the following normalization $\Sigma_k F_k = 1$.

The model equations (1), (3), (5), and (6) were solved numerically using the DVODE package [16].

2. RESULTS OF NUMERICAL CALCULATIONS

The model presented in previous section has been used to study properties of an Ar/C_2H_2 plasma afterglow and dust charge properties as functions of time for $n_{C2H2} = 5\times10^{13}$ cm^{-3} and n_e (t = 0) = 10^9 cm^{-3}. In Fig. 1, the electron and total positive and negative ion densities calculated using different approaches are shown.

One can see in Fig. 1 that for different afterglow times, the total negative ion density n_- obtained using the approach (ii) is smaller than n_- calculated in the case (i). This is because of the loss of all negative ions $C_{2n}H^-$ (considered by the model) in collisions with hydrogen atoms for the case (ii), while the loss of $C_{2n}H_2^-$ ions in collisions with H atoms is not taken into account in the case (i). Because of smaller n_-, the total density of positive ions in the case (ii) is smaller than in the case (i). The last conclusion also follows from the quasineutrality condition (Eq. (2)) and the fact that the time dependence for n_e is nearly the same in the both cases (i) and (ii) for $t \leq 0.5$ ms (see Fig. 1). At $t > 0.5$ ms, n_e decreases faster with time in the case (i) than in the case (ii).

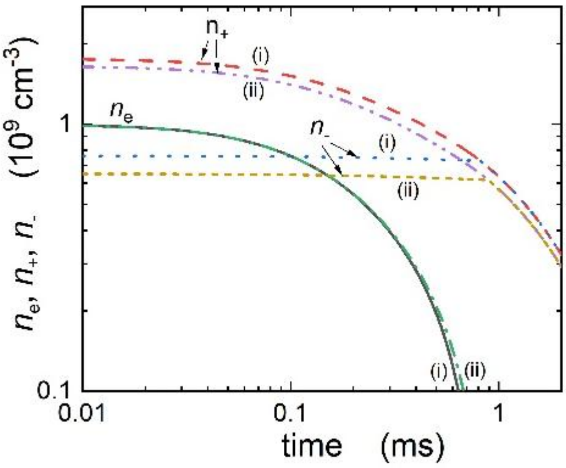

Fig. 1. The calculated electron (n_e), total positive ion ($n_+ = \sum_\alpha n_\alpha^+$) and total negative ion ($n_- = \sum_\alpha n_\alpha^-$) densities as functions of time in the Ar/C_2H_2 plasma afterglow in the cases (i) and (ii)

We also analyzed properties of the afterglow plasma using the approach (ii) and neglecting by the loss of negative ions in collisions with hydrogen atoms. For this case, the calculated time dependences for electron and total ion densities were found to be nearly the same as in the case (i) (therefore, they are not shown in Fig. 1).

The time dependences for negative ion densities in the afterglow are shown in Fig. 2. In the beginning of the afterglow (at $t \leq 1$ ms), the density of $C_2H_2^-$ anions obtained using the approach (i) is slightly larger than the C_2H^- density calculated using the approach (ii) because we do not account for the loss of $C_2H_2^-$ in collisions with H atoms. Since the loss of all $C_{2n}H_2^-$ anions in collisions with hydrogen atoms is not accounted in the case (i), the densities of these anions are larger than the corresponding densities of $C_{2n}H^-$ negative ions obtained using the approach (ii) (see Figs. 2,a and b).

Because of plasma quasineutrality and larger n_- in the case (i), the densities of different positive ions calculated in the case (ii) are smaller than the corresponding densities obtained in the case (i) (Fig. 3). This difference is also mainly due to the losses of $C_{2n}H^-$ anions in collisions with hydrogen atoms, which are taken into account in the case (ii) (see Table 2). The time dependences for the densities of different positive ions calculated in the case (ii) with neglecting by the loss of negative ions in collisions with H atoms were found to be nearly the same as those obtained in the case (i).

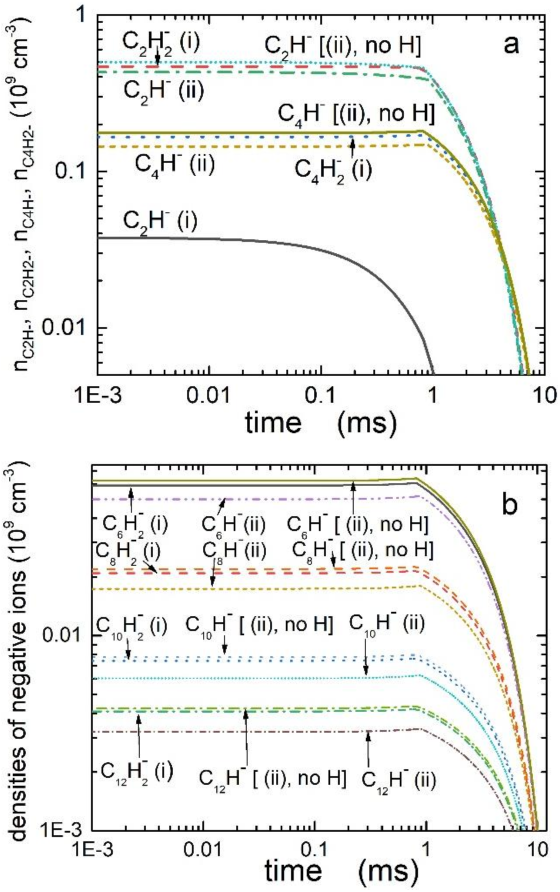

Fig. 2. The densities of different negative ions calculated in the cases (i) and (ii) and in the case (ii) with neglecting he loss of negative ions in collisions with H atoms [(ii), no H]

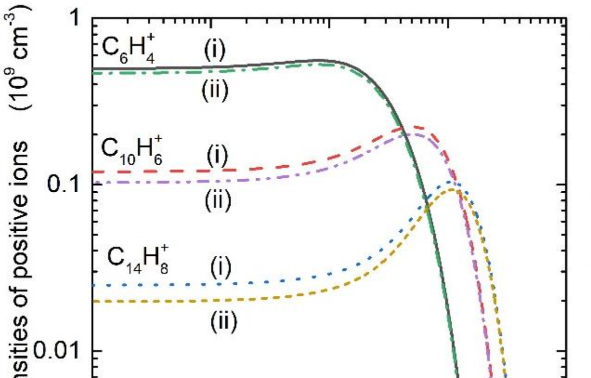

Fig. 3. The time dependences for the densities of $C_6H_4^+$, $C_{10}H_6^+$, and $C_{14}H_8^+$ ions calculated in the cases (i) and (ii)

We also calculated the mean dust charge as a function of time for a_d =100 nm at different assumptions (Fig. 4,a). It has been found that $|Z_d|$ decreases slightly faster with increasing the afterglow time in the case (i) than in the case (ii). The faster discharging in the case (i) is mainly due to larger ion densities in the case (i) (see Figs. 1 and 3).

The variance at $t \geq 1$ ms decreases faster with time in the case (i) comparing with the case (ii) (see Fig. 4,b) because of smaller $|Z_d|$ in the former case (see Fig. 4,a).

In Fig. 4,c, the dust charge distribution functions (DCDFs) obtained from Eq. (6) for a_d = 100 nm in the late afterglow (at t = 5.05 ms) are shown. The DCDF calculated in the case (ii) is slightly shifted to the region of larger $|Z^k_d|$ comparing with the dust charge distribution obtained in the case (i). It was found that Z_d, σ^2_z and F_k obtained in the case (i) are very similar to the corresponding values calculated in the case (ii) with neglecting by interaction of negative ions with hydrogen atoms. Moreover, the DCDFs obtained from Eq. (6) can be well approximated by the Gaussian distributions calculated using Eq. (4) [8].

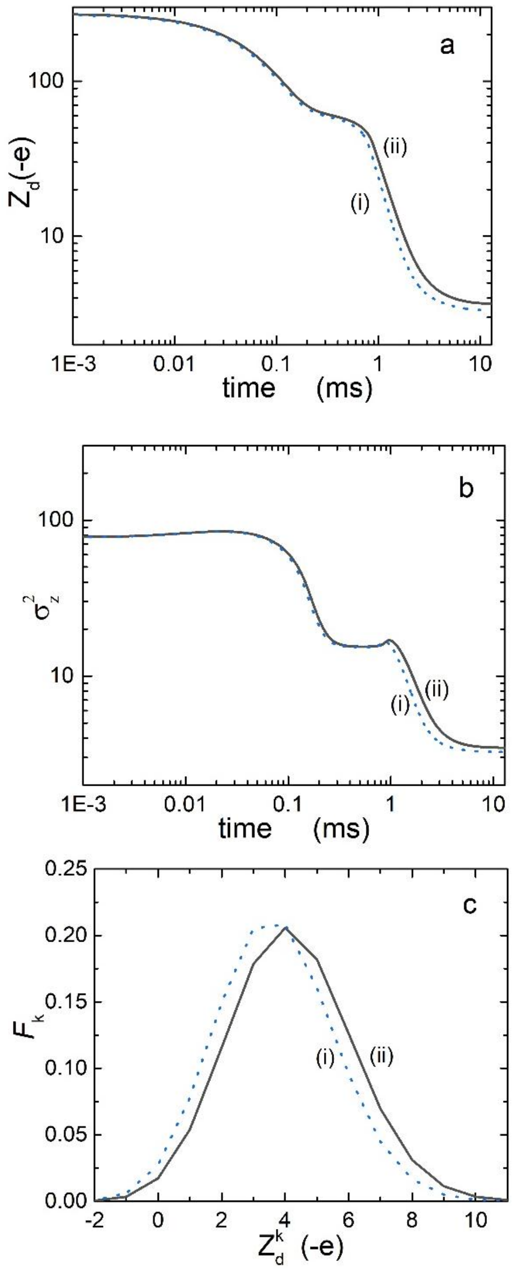

Fig. 4. $|Z_d|$ (a), σ^2_z (b) as functions of time and F_k (c) at t = 5.05 ms for a_d =100 nm

SUMMARY

Thus, it has been shown how the description of negative ion formation in an Ar/C_2H_2 dusty plasma afterglow affects the numerical results on the electron and ion densities, dust charge and dust charge distribution function. Two typical pathways of formation of anions in the plasma have been considered. The afterglow plasma properties calculated in the case, when $C_{2n}H_2^-$ negative ions are the dominant anions in the plasma afterglow (the case (i)), have been compared with the properties obtained in the case when $C_{2n}H^-$ anions are only the negative ions in the afterglow plasma (the case (ii)). It has been found that the time dependences for the densities of electrons, positive ions, mean dust charge and its variance obtained in the both cases are similar. The differences between the dependences obtained in the cases (i) and (ii) are mainly due to the losses of $C_{2n}H^-$ anions in collisions with hydrogen atoms, which are taken into account by this model in the case (ii).

The results presented here are relevant to many applications involving low-temperature plasmas [17-20], especially gas discharges used for the synthesis of various nanostructures.

REFERENCES

1. I.B. Denysenko, K. Ostrikov, N.A. Azarenkov. *Modelling of plasma-assisted growth of vertically aligned carbon nanostructures* / M.C. Wythers, editor. Advances in Materials Science Research, v. 34, New York: «Nova Science Publishers Inc.», 2018, p. 1-57.
2. I.B. Denysenko, S. Xu, J.D. Long, P.P. Rutkevych, N.A. Azarenkov, K. Ostrikov // *J. Appl. Phys.* 2004, v. 95, p. 2713.
3. V. Lisovskiy, A. Minenkov, S. Dudin, S. Bogatyrenko, P. Platonov, V. Yegorenkov // *ACS Omega*. 2022, v. 7, p. 47941.
4. K. De Bleecker, A. Bogaerts, W. Goedheer // *Phys. Rev. E.* 2006, v. 73, p. 026405.
5. M. Mao, J. Benedikt, A. Consoli, A. Bogaerts // *J. Phys. D: Appl. Phys*. 2008, v. 41, p. 225201.
6. M. Jiménez-Redondo, I. Tanarro, R.J. Peláez, L.Díaz-Pérez, V.J. Herrero // *J. Phys. Chem. A.* 2019, v. 123, p. 8135.
7. M. Jiménez-Redondo, I. Tanarro, V.J. Herrero // *Plasma Sources Sci. Technol.* 2022, v. 31, p. 065003.
8. I.B. Denysenko, M. Mikikian, N.A. Azarenkov // *J. Phys. D: Appl. Phys.* 2024, v. 57, p. 145202.
9. M. Jiménez-Redondo, I. Tanarro, V.J. Herrero // *Plasma Sources Sci. Technol.* 2024, v. 33, p. 039501.
10. I.B. Denysenko, E. von Wahl, M. Mikikian, J. Berndt, S. Ivko, H. Kersten, E. Kovacevic, N.A. Azarenkov // *J. Phys. D: Appl. Phys.* 2020, v. 53, p. 135203.
11. C. Barckholtz, T.P. Snow, V.M. Bierbaum // *Astrophys. J*. 2001, v. 547, p. L171.
12. I.B. Denysenko, I. Stefanović, M. Mikikian, E. Kovacevic, J. Berndt // *J. Phys. D: Appl. Phys.* 2021, v. 54, p. 065202.
13. A. Bouchoule. *Dusty Plasmas: Physics, Chemistry, and Technological Impacts in Plasma Processing*. New York: “Wiley”, 1999, 424 p.
14. B. Shotorban // *Phys. Rev. E.* 2011, v. 83, p. 066403.
15. T. Matsoukas, M. Russell, M. Smith // *J. Vac. Sci. Technol. A.* 1996, v. 14, p. 624.
16. P.N. Brown, G.D. Byrne, A.C. Hindmarsh // *SIAM J. Sci. Stat. Comput.* 1989, v. 10, p**.** 1038.
17. A.F. Tseluyko, V.T. Lazuryk, D.V. Ryabchikov, V.I. Maslov, N.A. Azarenkov, I.N. Sereda, D.V. Zinov'ev, N.N. Yunakov, A.A. Makienko // *Problems of Atomic Science and Technology. Series “Plasma Physics”.* 2009, № 1, p. 165.
18. I.O. Girka, I.V. Pavlenko, M. Thumm // *Phys. Plasmas*. 2018, v. 25, p. 052109.
19. I.B. Denysenko, H. Kersten, N.A. Azarenkov // *Phys. Rev. E.* 2015, v. 92, p. 033102.
20. B. Sikimić, I. Stefanović, I.B. Denysenko, J. Winter // *Plasma Sources Sci. Technol.* 2013, v. 22, p. 045009.

Article received 30.10.2024

РІЗНІ ПІДХОДИ ДО ОПИСУ УТВОРЕННЯ НЕГАТИВНИХ ІОНІВ У ПІСЛЯСВІТІННІ АРГОН-АЦЕТИЛЕНОВОЇ ПЛАЗМИ

І.Б. Денисенко, М.О. Азарєнков, В. Вінніченко, Г. Бурмака

Досліджено властивості Ar/C_2H_2 плазми з порошинками, що є у режимі післясвітіння, за різних припущень щодо утворення негативних іонів. По-перше, числові розрахунки виконано за припущення, що негативні іони $C_{2n}H_2^-$, де *n* – це натуральне число, є домінантними аніонами в післясвітінні цієї плазми (випадок (i)). По-друге, дослідження проведено за припущення, що аніони $C_{2n}H^-$ є єдиними негативними іонами, які присутні у цій плазмі післясвітіння (випадок (ii)). Показано, що сумарна густина негативних іонів n_- у випадку (ii) менша, ніж n_-, що розрахована у випадку (i). Завдяки меншій n_- концентрації позитивних іонів менші, а абсолютні значення середнього заряду порошинок та його дисперсії більші у випадку (ii), ніж відповідні значення, які розраховано за допомогою підходу (i). Було також обчислено функції розподілу порошинок за зарядом (ФРПЗ) за пізніх часів післясвітіння. Встановлено, що ФРПЗ, які розраховано у випадку (ii), зміщені в область більших негативних зарядів порівняно з ФРПЗ, які було отримано у випадку (i). Ці відмінності зумовлені переважно втратами $C_{2n}H^-$ аніонів у зіткненнях з атомами водню у випадку (ii). У випадку, якщо в моделях не враховуються втрати негативних іонів у зіткненнях з атомами водню, обидва підходи дають майже однакові часові залежності для густин позитивних та негативних іонів, електронної густини, середнього заряду порошинок та його дисперсії.